Bol. Soc. Paran. Mat.
©SPM – E-ISSN-2175-1188
SPM: www.spm.uem.br/bspm

(3s.) **v. 2025 (43) 1** : 1–15.
ISSN-0037-8712
doi:10.5269/bspm.75295

Finite-Time Synchronization in a Novel Discrete Fractional SIR Model for COVID-19

Iqbal M. Batiha[1,2], Issam Bendib[3], Adel Ouannas[4], Praveen Agarwal*[2,5], Nidal Anakira[6,7], Iqbal H. Jebril[1] and Shaher Momani[2,8]

ABSTRACT: This paper proposes a novel discrete fractional-order (FO) SIR model to capture the complex transmission dynamics of COVID-19. By incorporating memory effects via Caputo fractional difference operators, the model extends the classical SIR framework to account for nonlocal interactions and historical dependencies inherent in epidemic data. A master-slave configuration is introduced, and sufficient conditions for finite-time synchronization (FTSY) between these systems are derived using the Lyapunov stability theory and the discrete Mittag–Leffler function. The analysis demonstrates that, under appropriate control laws, the error dynamics between the master and slave systems converge to zero within a finite settling time. Numerical simulations are provided to validate the theoretical findings, illustrating the impact of various parameters on the evolution of susceptible, infected, and recovered populations. The integration of fractional calculus in this discrete framework enhances the accuracy of epidemic predictions and offers a robust control strategy for coordinating interventions across different regions.

Key Words: Discrete fractional calculus, Finite-time synchronization, Lyapunov stability, epidemic modeling.

Contents

1. Introduction

In 2020, the World Health Organization (WHO) declared COVID-19 a global pandemic, resulting in a devastating loss of life, with reported global deaths exceeding 5 million. Various preventive measures, such as mask-wearing, sanitization, and enforced quarantine protocols, were implemented worldwide [1]. From a mathematical perspective, developing accurate models to describe the spread and impact of the COVID-19 pandemic is essential [2,3]. One of the most widely recognized frameworks for this purpose is the Susceptible-Infectious-Recovered (SIR) model, which effectively captures the dynamics of infectious diseases and evaluates different transmission scenarios. The SIR model is useful for assessing the efficacy of various intervention strategies. It consists of a system of ordinary differential equations that categorize the total population into compartments representing susceptibility, infection-related mortality, and recovery over a specified period [4].

In mathematical modeling, ODEs are typically employed for continuous-time systems, while difference equations are utilized for discrete-time systems. A notable example is the development of a time-dependent SIR model presented in [5], which analyzed the transmission rate of COVID-19 across different regions of India. Utilizing ArcGIS 10.2, district-wise spatial distribution maps were created to examine the effects of complete lockdowns on the virus's spread. This mode and other pioneering works have significantly contributed to understanding COVID-19 transmission in continuous-time frameworks.

* Corresponding author

Submitted January 18, 2025. Published April 20, 2025
2010 *Mathematics Subject Classification:* 35B40, 35L70.

Recently, discrete-time models have gained prominence in the study of infectious diseases, primarily due to the nature of pandemic data, which is often recorded at discrete intervals [6]. For instance, random walk models for daily time series of confirmed COVID-19 cases in various countries were introduced in [7], where the models incorporated evolutionary equations with memory functions to account for non-ergodic fields observed in COVID-19 data. Additionally, [8] applied mathematical modeling to analyze the spread and treatment of several infectious diseases, including COVID-19, in its SIR form.

In this context, FO models have emerged as powerful tools in epidemiological studies [9,10,11]. A FO SIR model based on a continuous-time random walk was developed, introducing time-since-infection dependencies for both infectivity and recovery [12,13,14,15,16,17]. Another FO-SIR model proposed by Naik focused on global dynamics [18,19,20]. Moreover, in [21], a generalized FO-SIR model was designed to predict the spread of COVID-19 using the Grünwald-Letnikov nabla FO difference operator for time-domain implementation [22,23]. Furthermore, vaccination strategies have been integrated into various discrete-time models. For instance, Xiang et al. [24] examined a discrete-time epidemic model with vaccination, focusing on its dynamic behavior. Bifurcations and stability in a discrete-time susceptible-infected-susceptible (SIS) model with vaccination were explored in [25]. A discrete SIR epidemic model with a constant vaccination strategy was also analyzed for its dynamical properties. Readers interested in a broader overview of discrete-time models can refer to [26], which illustrates that models often exhibit more complex dynamics than their continuous-time counterparts.

The concept of FTSY in discrete FO systems, including those modeling the COVID-19 pandemic, refers to the phenomenon where a set of dynamical systems converge to a common state within a finite period [27,28,29,30,31,32,33,34,35,36,37,38,39]. For a discrete FO COVID-19 system, this typically involves the following key components:

- The COVID-19 dynamics can be modeled using a set of FO difference equations that describe the interaction among susceptible, infected, and recovered populations. The FO reflects memory effects and non-local interactions.
- The goal is for multiple discrete FO systems, each representing a different population or region, to synchronize their states (e.g., the number of infected individuals) despite potential differences in their initial conditions or parameter values.
- Synchronization is achieved within a predetermined, finite time T, meaning that there exists a time $t \leq T$ such that the states of all systems converge to a common trajectory or state.
- To facilitate FTSY, control strategies (e.g., state feedback controllers) can be designed based on Lyapunov's stability theory. These strategies aim to minimize the difference between the states of the synchronized systems.
- Sufficient conditions for FTSY may involve the application of Lyapunov functions, which help establish the stability of the synchronization process and ensure that the systems converge to the desired state within the specified time.

This work aims to contribute to the epidemiological modeling of COVID-19 by proposing a novel FO discrete-time model. To our knowledge, FO discrete-time models for COVID-19 have not been extensively explored, motivating this study due to the predominant focus on continuous-time models in previous works. For instance, delayed incommensurate FO-SIR models were studied for bifurcation control and stability [40], while [12] concentrated on numerical simulations for FO-SIR models. Over the past few years, numerous SIR models based on FO differential equations have been developed in epidemiology [41,42,43]. The key objectives of this research paper include:

- Constructing a mathematical model to predict the behavior of COVID-19, categorizing the population into susceptible (S), infected (I), recovered (R), and deceased (D) groups.
- Utilizing FO calculus to capture memory effects and non-local interactions in the dynamics of disease transmission, which traditional models might overlook.

- Investigating the conditions necessary for multiple FO-SIR systems to synchronize their dynamics, assessing stability and the impact of network topology on synchronization.
- Employing Lyapunov functions to derive conditions that ensure FTSY, providing a framework to guarantee the convergence of state variables to a common trajectory.
- Validating the model and synchronization strategies through simulations to demonstrate how various parameters influence the system's dynamics.
- Offering insights applicable to real-world scenarios, such as controlling disease outbreaks and optimizing vaccination strategies.
- Identifying challenges such as parameter estimation and the robustness of synchronization in uncertain environments while proposing future research directions to improve synchronization techniques in more complex epidemic models.

This paper is organized as follows: Section 2 introduces and formalizes key concepts related to FO and discrete calculus. Section 3 studies the formulation of a mathematical model to understand and predict the dynamics of COVID-19, focusing on creating a discrete FO-SIR model that categorizes the population into susceptible (S), infected (I), recovered (R), and deceased (D) groups. Section 4 examines the synchronization behavior of discrete FO SIR models, investigating how interconnected systems modeling the spread of infectious diseases can align their state variables rapidly over a FTSY. Finally, Section 5 applies theoretical stability results to numerical examples based on a discrete COVID-19 model.

2. Mathematical Background

This section introduces various concepts about FO and variable discrete calculus. Let $\mathrm{a}, \mathrm{T} \in \mathbb{R}$. We denote the set of natural numbers starting from a as follows:

$$\mathbb{N}_{\mathrm{a}} = \{\mathrm{a}, \mathrm{a}+1, \mathrm{a}+2, \ldots\}.$$

Additionally, we define the set of natural numbers from a to T as:

$$\mathbb{N}_{\mathrm{a}}^{\mathrm{T}} = \{\mathrm{a}, \mathrm{a}+1, \mathrm{a}+2, \ldots, \mathrm{T}\}.$$

Definition 2.1 ([1]) *Let $\mu > 0$. The FO sum of a function $h\colon \mathbb{N}_a \to \mathbb{R}$ is defined by*

$$\Delta_{\mathrm{a}}^{-\mu}\mathrm{h}(\mathrm{t}) = \frac{1}{\Gamma(\mu)} \sum_{\mathrm{s}=\mathrm{a}}^{\mathrm{t}-\mu} \big(\mathrm{t}-\mathrm{s}-1\big)^{\mu-1}\mathrm{h}(\mathrm{s}), \quad \mathrm{t} \in \mathbb{N}_{\mathrm{a}+\mu}. \tag{2.1}$$

Here, $\Gamma(\cdot)$ denotes Euler's gamma function,

$$\Gamma(\mu) = \int_0^{\infty} \mathrm{t}^{\mu-1}\mathrm{e}^{-\mathrm{t}}\,\mathrm{dt}, \tag{2.2}$$

and the generalized factorial is given by

$$\mathrm{t}^{(\mu)} = \frac{\Gamma(\mathrm{t}+1)}{\Gamma(\mathrm{t}+1-\mu)}. \tag{2.3}$$

Definition 2.2 ([1]) *For a function $h\colon \mathbb{N}_a \to \mathbb{R}$, the μ-th order Caputo fractional difference operator is defined as*

$${}^{\mathrm{C}}\Delta_{\mathrm{a}}^{\mu}\mathrm{h}(\mathrm{t}) = \begin{cases} \Delta_a^{-(1-\mu)}\Delta h(t) = \dfrac{1}{\Gamma(1-\mu)} \displaystyle\sum_{s=a}^{t-(1-\mu)} (t-s-1)^{-\mu}\,\Delta h(s), & \text{if } 0 < \mu < 1, \\ \Delta h(t), & \text{if } \mu = 1. \end{cases} \tag{2.4}$$

Here, $t \in \mathbb{N}_{a+1-\mu}$.

Definition 2.3 ([1]) *Let $h\colon \mathbb{N}_a \to \mathbb{R}$ be a function. Then, for all $t \in \mathbb{N}_a$, the following identity holds:*

$$\Delta^{-\mu}_{a+(1-\mu)}\, {}^{C}\Delta^{\mu}_{a} h(t) = h(t) - h(a). \tag{2.5}$$

Definition 2.4 ([44]) *Let $\Lambda \in \mathbb{R}$ and $\mu, t \in \mathbb{R}^{*+}$. The discrete Mittag-Leffler function is defined by*

$$E_{\mu}(\Lambda, t) = \sum_{k=0}^{\infty} \Lambda^{k} \frac{\Big(t + (k-1)(\mu-1)\Big)^{(k\mu)}}{\Gamma(\mu k + 1)}. \tag{2.6}$$

We consider the following linear fractional difference equation with a fractional delay:

$$\begin{cases} {}^{C}\Delta^{\mu}_{a}\Theta(t) = \Lambda\, \Theta(t+\mu), \quad t \in \mathbb{N}_{a+1-\mu}, \quad |\Lambda| < 1, \\ \Theta(a) = \Theta_a. \end{cases} \tag{2.7}$$

Definition 2.5 ([45]) *System (2.7) is finite–time stable with respect to $\{\zeta, \varepsilon, J\}$ if*

$$\|\Theta_a\| < \zeta \quad \textit{implies} \quad \|\Theta(t)\| < \varepsilon, \quad \forall\, t \in J. \tag{2.8}$$

Lemma 2.1 ([45]) *The linear fractional difference equation (2.7) admits a unique solution expressed in terms of the discrete Mittag–Leffler function:*

$$\Theta(t) = \Theta_a\, E_{\mu}(\Lambda, t). \tag{2.9}$$

Theorem 2.1 ([45]) *Let $\vartheta(t)$ and $\chi(t)$ be nonnegative, nondecreasing discrete functions with $\chi(t) \geq M$ for all $t \in J$. Suppose that the following FO sum inequality holds:*

$$\Theta(t) \leq \vartheta(t) + \chi(t)\, \Delta^{-\mu}_{a+1-\mu}\Theta(t+\mu), \quad t \in \mathbb{N}_{a+1}. \tag{2.10}$$

Then, it follows that

$$\Theta(t) \leq \vartheta(t)\, E_{\mu}(\chi(t), t). \tag{2.11}$$

3. A Novel Discrete Fractional SIR Model for COVID-19 Dynamics

In this section, we introduce a novel discrete fractional SIR model that captures the complex dynamics of COVID-19 transmission. Traditional integer-order models, although useful, often fail to account for intrinsic memory effects. Moreover, non-local interactions play a significant role in disease spread. Our model incorporates the Caputo fractional difference operator, which effectively integrates historical dependencies. This integration results in a more accurate and realistic representation of the epidemic's evolution. The key parameters governing the dynamics of the proposed model are summarized in Table 1.

Table 1: Description of the model's parameters

Parameter	Description
η	Death rate due to COVID-19
δ	Natural death rate
ν	Number of new births
$\mathfrak{d}$	Infection rate
$\mathfrak{b}$	Recovery rate
ρ	Rate at which a recovering individual is at risk of reinfection

Following [1], the transmission dynamics of the proposed FO discrete SIR model are described by the following nonlinear system:

$$\begin{cases} \mathrm{S}(\mathrm{t}+1) = \mathrm{S}(\mathrm{t}) + \nu + \rho \mathrm{R}(\mathrm{t}) - \mathfrak{d}\mathrm{S}(\mathrm{t})\mathrm{I}(\mathrm{t}) - \delta \mathrm{S}(\mathrm{t}), \\ \mathrm{I}(\mathrm{t}+1) = \mathrm{I}(\mathrm{t}) + \mathfrak{d}\mathrm{S}(\mathrm{t})\mathrm{I}(\mathrm{t}) - (\eta + \delta + \mathfrak{b})\mathrm{I}(\mathrm{t}), \\ \mathrm{R}(\mathrm{t}+1) = \mathrm{R}(\mathrm{t}) + \mathfrak{b}\mathrm{I}(\mathrm{t}) - (\delta + \rho)\mathrm{R}(\mathrm{t}), \\ \mathrm{D}(\mathrm{t}+1) = \mathrm{D}(\mathrm{t}) + \mu \mathrm{I}(\mathrm{t}). \end{cases} \tag{3.1}$$

The system is subject to the initial conditions (ICs):

$$\mathrm{S}(0) = \mathrm{S}_0, \quad \mathrm{I}(0) = \mathrm{I}_0, \quad \mathrm{R}(0) = \mathrm{R}_0. \tag{3.2}$$

Note that the first three equations do not involve the D class. Therefore, the D class can be analyzed independently using

$$\mathrm{N}(\mathrm{t}) = \mathrm{S}(\mathrm{t}) + \mathrm{I}(\mathrm{t}) + \mathrm{R}(\mathrm{t}) + \mathrm{D}(\mathrm{t}). \tag{3.3}$$

As a result, the last equation of system (3.1) can be omitted, allowing us to focus on the first three equations.

Moreover, note that the parameter $\mathfrak{d}$ is very small. It is defined as

$$\mathfrak{d} = \frac{\mathfrak{p}\mathfrak{k}}{N},$$

where $\mathfrak{k}$ is the contact rate per unit time ($0 \leq \mathfrak{k} \leq 1$), $\mathfrak{p}$ is the probability of contagion ($0 \leq \mathfrak{p} \leq 1$), and N is the total population (typically tens of thousands or more). Consequently, the terms $\mathfrak{d}S(t)$ and $\mathfrak{d}I(t)$ are also relatively small.

Although our model does not explicitly address age groups and vaccination, this omission does not imply neglect. High life expectancy contributes to an elevated death rate. Furthermore, while vaccination does not provide 100% immunity, it reduces the likelihood of infection (thereby decreasing $\mathfrak{d}$), lowers virus mortality (represented by ρ), and increases the recovery rate (denoted by $\mathfrak{b}$).

Based on the nonlinear model in equation (3.3), we now introduce the fractional-order model that is the focus of this study. The model is given by:

$$\begin{cases} {}^{\mathrm{C}}\Delta_{\mathrm{a}}^{\mu}\mathrm{S}(\mathrm{t}) = \nu + \rho \mathrm{R}(\mathrm{t}+\mu-1) - \mathfrak{d}\mathrm{S}(\mathrm{t}+\mu-1)\mathrm{I}(\mathrm{t}+\mu-1) - \delta \mathrm{S}(\mathrm{t}+\mu-1), \\ {}^{C}\Delta_{a}^{\mu} I(t) = \mathfrak{d}S(t+\mu-1)I(t+\mu-1) - (\eta + \delta + \mathfrak{b})I(t+\mu-1), \\ {}^{C}\Delta_{a}^{\mu} R(t) = \mathfrak{b}I(t+\mu-1) - (\delta + \rho)R(t+\mu-1), \end{cases} \tag{3.4}$$

with the initial conditions

$$\mathrm{S}(0) = \mathrm{S}_0, \quad \mathrm{I}(0) = \mathrm{I}_0, \quad \mathrm{R}(0) = \mathrm{R}_0.$$

Here, $0 < \mu < 1$ and $t \in \mathbb{N}_{1-\mu}$. In the following analysis, we highlight a significant finding regarding the stability of the solution to the system in equation (3.4).

4. Finite-Time Synchronization of Discrete Fractional SIR Models

This section investigates FTSY in discrete fractional SIR models. It emphasizes the rapid alignment of state variables in interconnected systems modeling infectious disease spread. By employing FO calculus, the model captures memory effects and complex transmission dynamics.

We define the slave system as follows:

$$\begin{cases} {}^{\mathrm{C}}\Delta_{\mathrm{a}}^{\mu}\hat{\mathrm{S}}(\mathrm{t}) = \nu + \rho \hat{\mathrm{R}}(\mathrm{t}+\mu-1) - \mathfrak{d}\hat{\mathrm{S}}(\mathrm{t}+\mu-1)\hat{\mathrm{I}}(\mathrm{t}+\mu-1) - \delta \hat{\mathrm{S}}(\mathrm{t}+\mu-1) + \hat{\mathrm{C}}_1, \\ {}^{\mathrm{C}}\Delta_{\mathrm{a}}^{\mu}\hat{\mathrm{I}}(\mathrm{t}) = \mathfrak{d}\hat{\mathrm{S}}(\mathrm{t}+\mu-1)\hat{\mathrm{I}}(\mathrm{t}+\mu-1) - (\eta + \delta + \mathfrak{b})\hat{\mathrm{I}}(\mathrm{t}+\mu-1) + \hat{\mathrm{C}}_2, \\ {}^{\mathrm{C}}\Delta_{\mathrm{a}}^{\mu}\hat{\mathrm{R}}(\mathrm{t}) = \mathfrak{b}\hat{\mathrm{I}}(\mathrm{t}+\mu-1) - (\delta + \rho)\hat{\mathrm{R}}(\mathrm{t}+\mu-1) + \hat{\mathrm{C}}_3, \end{cases} \tag{4.1}$$

Subject to the following ICs:

$$\hat{\mathrm{S}}(0) = \hat{\mathrm{S}}_0, \quad \hat{\mathrm{I}}(0) = \hat{\mathrm{I}}_0, \quad \hat{\mathrm{R}}(0) = \hat{\mathrm{R}}_0. \tag{4.2}$$

Define the error system as

$$\mathrm{e(t)} = \begin{pmatrix} \hat{\mathrm{S}}(\mathrm{t}) - \mathrm{S(t)} \\ \hat{\mathrm{I}}(\mathrm{t}) - \mathrm{I(t)} \\ \hat{\mathrm{R}}(\mathrm{t}) - \mathrm{R(t)} \end{pmatrix}. \tag{4.3}$$

Using the slave system (4.1) and the master system, we derive the error dynamics:

$$\begin{cases} {}^{\mathrm{C}}\Delta_{\mathrm{a}}^{\mu}\mathrm{e}_1(\mathrm{t}) = & \rho\, e_3(t+\mu-1) - \mathfrak{d}\Big(\hat{S}(t+\mu-1)\hat{I}(t+\mu-1) - S(t+\mu-1)I(t+\mu-1)\Big) \\ & -\delta\, e_1(t+\mu-1) + \hat{C}_1, \\ {}^{\mathrm{C}}\Delta_{\mathrm{a}}^{\mu}\mathrm{e}_2(\mathrm{t}) = & \mathfrak{d}\Big(\hat{S}(t+\mu-1)\hat{I}(t+\mu-1) - S(t+\mu-1)I(t+\mu-1)\Big) \\ & -(\eta+\delta+\mathfrak{b})e_2(t+\mu-1) + \hat{C}_2, \\ {}^{\mathrm{C}}\Delta_{\mathrm{a}}^{\mu}\mathrm{e}_3(\mathrm{t}) = & \mathfrak{b}\, e_2(t+\mu-1) - (\delta+\rho)e_3(t+\mu-1) + \hat{C}_3, \end{cases} \tag{4.4}$$

with the error ICs:

$$\mathrm{e}_1(0) = \hat{\mathrm{S}}_0 - \mathrm{S}_0, \quad \mathrm{e}_2(0) = \hat{\mathrm{I}}_0 - \mathrm{I}_0, \quad \mathrm{e}_3(0) = \hat{\mathrm{R}}_0 - \mathrm{R}_0. \tag{4.5}$$

Definition 4.1 ([46,47]) *Master-slave systems (3.4) and (4.1) are said to be FTSY if there exists a controller* $\mathrm{C_i(t)}$, $(i = 1, 2, 3)$, *and a constant* $T > 0$ *such that*

$$\lim_{\mathrm{t}\to\mathrm{T}} \|\mathrm{e(t)}\|_1 = 0, \tag{4.6}$$

and

$$\|\mathrm{e(t)}\|_1 = \|\hat{\mathrm{S}}(\mathrm{t}) - \mathrm{S(t)}\|_1 + \|\hat{\mathrm{I}}(\mathrm{t}) - \mathrm{I(t)}\|_1 + \|\hat{\mathrm{R}}(\mathrm{t}) - \mathrm{R(t)}\|_1 \equiv 0, \tag{4.7}$$

for all $t > T$. *Here,* $(S(t), I(t), R(t))^T$ *and* $\left(\hat{S}(t), \hat{I}(t), \hat{R}(t)\right)^T$ *are the solutions of the master system (3.4) and the slave system (4.1) with initial conditions* $(S_0, I_0, R_0)^T$ *and* $\left(\hat{S}_0, \hat{I}_0, \hat{R}_0\right)^T$, *respectively. The constant* T *is called the settling time.*

Theorem 4.1 *The master-slave system given by (3.4) and (4.1) achieves FTSY under the following control strategies:*

$$\begin{cases} \mathrm{C}_1(\mathrm{t}) = -\rho\, \mathrm{e}_3(\mathrm{t}+\mu-1), \\ \mathrm{C}_2(\mathrm{t}) = 0, \\ \mathrm{C}_3(\mathrm{t}) = -\mathfrak{b}\, \mathrm{e}_2(\mathrm{t}+\mu-1). \end{cases} \tag{4.8}$$

This synchronization is achieved provided that

$$\mathrm{E}_{\mu}\Big(\max\{\eta+\delta+\mathfrak{b},\, \delta+\rho\}, \mathrm{t}\Big) < \frac{\varepsilon}{\zeta}. \tag{4.9}$$

Proof: Substitute the control laws (4.8) into the error dynamics (4.4) to obtain:

$$\begin{cases} {}^{\mathrm{C}}\Delta_{\mathrm{a}}^{\mu}\mathrm{e}_1(\mathrm{t}) = -\delta\, \mathrm{e}_1(\mathrm{t}+\mu-1) - \mathfrak{d}\Big(\hat{\mathrm{S}}(\mathrm{t}+\mu-1)\hat{\mathrm{I}}(\mathrm{t}+\mu-1) - \mathrm{S}(\mathrm{t}+\mu-1)\mathrm{I}(\mathrm{t}+\mu-1)\Big), \\ {}^{C}\Delta_{a}^{\mu}e_2(t) = \mathfrak{d}\Big(\hat{S}(t+\mu-1)\hat{I}(t+\mu-1) - S(t+\mu-1)I(t+\mu-1)\Big) + (\eta+\delta+\mathfrak{b})\, e_2(t+\mu-1), \\ {}^{C}\Delta_{a}^{\mu}e_3(t) = -(\delta+\rho)\, e_3(t+\mu-1). \end{cases} \tag{4.10}$$

Using Definition 2.3, the solutions of (4.10) can be written as:

$$\begin{cases} e_1(t) = & e_1(0) - \Delta_{a+1-\mu}^{-\mu}\Big[\delta\, e_1(t+\mu-1) + \mathfrak{d}\Big(\hat{S}(t+\mu-1)\hat{I}(t+\mu-1) - S(t+\mu-1)I(t+\mu-1)\Big)\Big], \\ e_2(t) = & e_2(0) + \Delta_{a+1-\mu}^{-\mu}\Big[\mathfrak{d}\Big(\hat{S}(t+\mu-1)\hat{I}(t+\mu-1) - S(t+\mu-1)I(t+\mu-1)\Big) \\ & +(\eta+\delta+\mathfrak{b})\, e_2(t+\mu-1)\Big], \\ e_3(t) = & e_3(0) - (\delta+\rho)\,\Delta_{a+1-\mu}^{-\mu}\, e_3(t+\mu-1). \end{cases} \tag{4.11}$$

Next, summing the error components yields:

$$\begin{aligned} \mathrm{e}_1(\mathrm{t}) + \mathrm{e}_2(\mathrm{t}) + \mathrm{e}_3(\mathrm{t}) = e_1(0) + e_2(0) + e_3(0) \\ + \Delta_{\mathrm{a}+1-\mu}^{-\mu}\Big[-\delta\, \mathrm{e}_1(\mathrm{t}+\mu-1) + (\eta+\delta+\mathfrak{b})\, \mathrm{e}_2(\mathrm{t}+\mu-1) - (\delta+\rho)\, \mathrm{e}_3(\mathrm{t}+\mu-1)\Big]. \end{aligned} \tag{4.12}$$

It follows that

$$\begin{aligned} \|\mathrm{e}_1(\mathrm{t})\|_1 + \|\mathrm{e}_2(\mathrm{t})\|_1 + \|\mathrm{e}_3(\mathrm{t})\|_1 &\le \|e_1(0)\|_1 + \|e_2(0)\|_1 + \|e_3(0)\|_1 \\ &\quad + \Delta_{\mathrm{a}+1-\mu}^{-\mu}\Big(\delta\, \|\mathrm{e}_1(\mathrm{t}+\mu-1)\|_1 + (\eta+\delta+\mathfrak{b})\, \|\mathrm{e}_2(\mathrm{t}+\mu-1)\|_1 \\ &\quad + (\delta+\rho)\, \|\mathrm{e}_3(\mathrm{t}+\mu-1)\|_1\Big) \\ &\le \|e_1(0)\|_1 + \|e_2(0)\|_1 + \|e_3(0)\|_1 \\ &\quad + \max\Big\{\eta+\delta+\mathfrak{b}, \delta+\rho\Big\}\times \\ &\quad \Delta_{\mathrm{a}+1-\mu}^{-\mu}\Big(\|\mathrm{e}_1(\mathrm{t}+\mu-1)\|_1 + \|\mathrm{e}_2(\mathrm{t}+\mu-1)\|_1 + \|\mathrm{e}_3(\mathrm{t}+\mu-1)\|_1\Big). \end{aligned} \tag{4.13}$$

Thus, we have:

$$\|\mathrm{e}(\mathrm{t})\|_1 \le \|\mathrm{e}(0)\|_1 + \max\Big\{\eta+\delta+\mathfrak{b}, \delta+\rho\Big\}\, \Delta_{\mathrm{a}+1-\mu}^{-\mu}\|\mathrm{e}(\mathrm{t}+\mu-1)\|_1. \tag{4.14}$$

Applying Theorem 2.1, we obtain:

$$\begin{aligned} \|\mathrm{e}(\mathrm{t})\|_1 &\le \|e(0)\|_1\, E_\mu\Big(\max\Big\{\eta+\delta+\mathfrak{b}, \delta+\rho\Big\}, t\Big) \\ &\le \zeta\, E_\mu\Big(\max\Big\{\eta+\delta+\mathfrak{b}, \delta+\rho\Big\}, t\Big). \end{aligned} \tag{4.15}$$

Thus, by Definitions 2.5 and 4.1, the master-slave systems (3.4) and (4.1) achieve finite-time synchronization. □

5. Modeling and Numerical Solutions for the Discrete Fractional COVID-19 Model

In this section, we demonstrate the application of the theoretical stability results to two numerical examples based on the discrete COVID-19 model. Because most FO difference equations lack analytical solutions, numerical and approximation methods are essential. We utilize a numerical approach for these equations and derive formulations specifically tailored to the delta variant of COVID-19.

The discrete FO master system (3.4) is solved as follows:

$$\begin{cases} S(n) = S(0) + \dfrac{1}{\Gamma(\mu)} \sum\limits_{j=1}^{n} \dfrac{\Gamma(n-j+\mu)}{\Gamma(n-j+1)} \left[\nu + \rho R(j-1) - \mathfrak{d} S(j-1) I(j-1) - \delta S(j-1)\right], \\ I(n) = I(0) + \dfrac{d}{\Gamma(\mu)} \sum\limits_{j=1}^{n} \dfrac{\Gamma(n-j+\mu)}{\Gamma(n-j+1)} \left[\mathfrak{d} S(j-1) I(j-1) - (\eta + \delta + \mathfrak{b}) I(j-1)\right], \\ R(n) = R(0) + \dfrac{1}{\Gamma(\mu)} \sum\limits_{j=1}^{n} \dfrac{\Gamma(n-j+\mu)}{\Gamma(n-j+1)} \left[\mathfrak{b} I(j-1) - (\delta + \rho) R(j-1)\right], \\ n > 0. \end{cases} \tag{5.1}$$

Likewise, the discrete FO slave system (4.1) is given by:

$$\begin{cases} \hat{S}(n) = \hat{S}(0) + \dfrac{1}{\Gamma(\mu)} \sum\limits_{j=1}^{n} \dfrac{\Gamma(n-j+\mu)}{\Gamma(n-j+1)} \left[\nu + \rho \hat{R}(j-1) - \mathfrak{d} \hat{S}(j-1) I(j-1) - \delta \hat{S}(j-1) - \rho e_3(j-1)\right], \\ \hat{I}(n) = \hat{I}(0) + \dfrac{d}{\Gamma(\mu)} \sum\limits_{j=1}^{n} \dfrac{\Gamma(n-j+\mu)}{\Gamma(n-j+1)} \left[\mathfrak{d} \hat{S}(j-1) \hat{I}(j-1) - (\eta + \delta + \mathfrak{b}) \hat{I}(j-1) + (\eta + \delta + \mathfrak{b}) e_2(j-1)\right], \\ \hat{R}(n) = \hat{R}(0) + \dfrac{1}{\Gamma(\mu)} \sum\limits_{j=1}^{n} \dfrac{\Gamma(n-j+\mu)}{\Gamma(n-j+1)} \left[\mathfrak{b} \hat{I}(j-1) - (\delta + \rho) \hat{R}(j-1) - \mathfrak{b} e_2(j-1)\right], \\ n > 0. \end{cases} \tag{5.2}$$

Finally, the discrete FO error system (4.10) is given by:

$$\begin{cases} e_1(n) = e_1(0) - \dfrac{1}{\Gamma(\mu)} \sum\limits_{j=1}^{n} \dfrac{\Gamma(n-j+\mu)}{\Gamma(n-j+1)} \left[\delta e_1(j-1) + d(\hat{S}(j-1)\hat{I}(j-1) - S(j-1)I(j-1))\right], \\ e_2(n) = e_2(0) + \dfrac{1}{\Gamma(\mu)} \sum\limits_{j=1}^{n} \dfrac{\Gamma(n-j+\mu)}{\Gamma(n-j+1)} \left[d\left(\hat{S}(j-1)\hat{I}(j-1) - S(j-1)I(j-1)\right) + (\eta + \delta + \mathfrak{b}) e_2(j-1)\right], \\ e_3(n) = e_3(0) - \dfrac{\delta + \rho}{\Gamma(\mu)} \sum\limits_{j=1}^{n} \dfrac{\Gamma(n-j+\mu)}{\Gamma(n-j+1)} e_3(j-1), \\ n > 0. \end{cases} \tag{5.3}$$

Table 2: Model Parameters and Their Descriptions

Parameter	Description	Value
η	Mortality rate attributed to COVID-19 infections	0.01
δ	Rate of natural mortality in the population	0.1
ν	Birth rate in the population per unit time	1
$\mathfrak{d}$	Rate of new infections in the susceptible population	0.35
$\mathfrak{b}$	Recovery rate of infected individuals	0.14
ρ	Probability of reinfection for recovered individuals	0.15
μ	Order of the fractional derivative	0.14905
h	Time step in the discrete evolution equation	0.1
N	Number of spatial points in the system	100

The ICs for the master and slave systems in (5.1) and (5.2) are:

$$\begin{cases} S(0) = 1.5, \quad I(0) = 1.25, \quad R(0) = 0.5, \\ \hat{S}(0) = 1, \quad \hat{I}(0) = 0.75, \quad \hat{R}(0) = 0.25, \end{cases} \tag{5.4}$$

and the ICs for the error system (5.3) are:

$$e_1(0) = -0.5, \quad e_2(0) = -0.5, \quad e_3(0) = -0.25. \tag{5.5}$$

We obtain the values:

$$\zeta = 1.26, \quad \varepsilon = 1.999268627717895, \tag{5.6}$$

and, according to Theorem 4.1, the condition (4.9) is verified:

$$\mathrm{E}_{0.14905}(0.25, \mathrm{t}) \leq \mathrm{E}_{0.14905}(0.25, 10) = 1.586524487152021 < 1.586721133109440. \tag{5.7}$$

Thus, the master-slave system defined by (3.4) and (4.1) achieves FTSY.

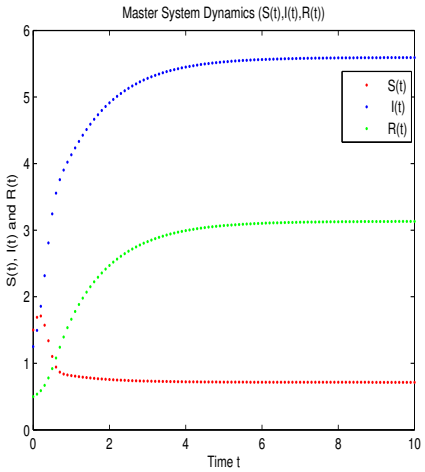

Figure 1: Simulation results for the master system: evolution of $S(t)$, $I(t)$, and $R(t)$.

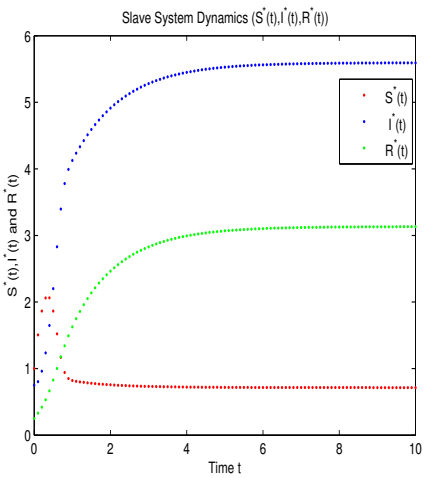

Figure 2: Simulation results for the slave system: evolution of $\hat{S}(t)$, $\hat{I}(t)$, and $\hat{R}(t)$.

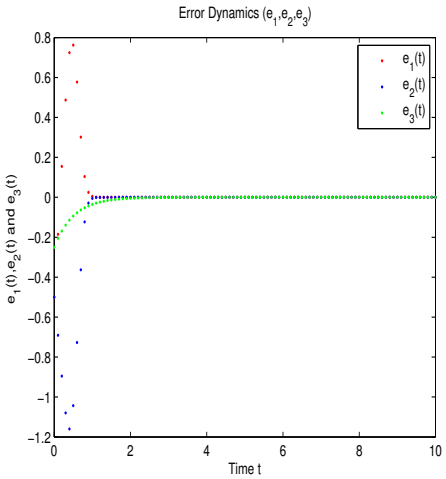

Figure 3: Simulation of error dynamics: evolution of $e_1(t)$, $e_2(t)$, and $e_3(t)$.

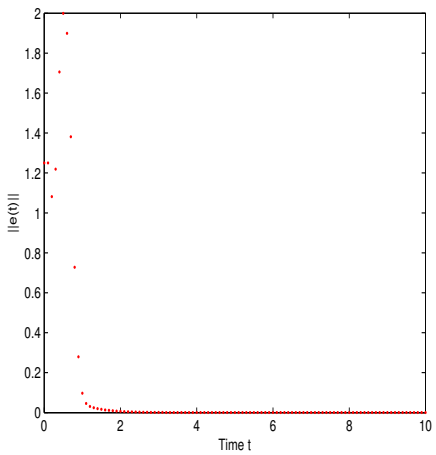

Figure 4: Estimation of the norm $\|e_1(t)\|$ over time.

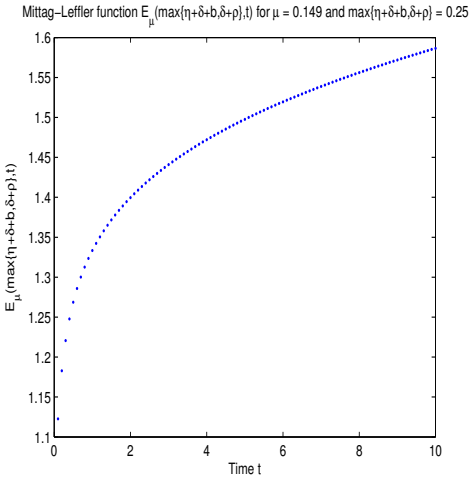

Figure 5: Estimation of the discrete Mittag–Leffler function $E_{0.14905}(0.25, t)$.

In this study, parameter values play a crucial role in defining system dynamics and determining whether finite-time synchronization between the master and slave systems is achieved. The fractional-order master, slave, and error systems are governed by parameters that capture various biological and epidemiological processes, directly influencing the evolution of susceptible, infected, and recovered populations over discrete time steps.

Key Roles of Parameter Values:

- **Model Parameters**
  - Parameters such as the infection rate $\mathfrak{d}$, recovery rate $\mathfrak{b}$, mortality rate η, and reinfection probability ρ determine the system's behavior by capturing real-world aspects of disease transmission, recovery, and demographic changes.
  - The fractional derivative order $\mu = 0.14905$ is critical, as it effectively captures memory effects and long-term dependencies in the system.
- **Initial Conditions**
  - The slight differences in initial conditions for the master and slave systems enable the analysis of synchronization dynamics.
- **Synchronization and Stability**
  - The synchronization condition from Theorem 4.1 relies on key values (e.g., $\zeta = 1.26$ and $\varepsilon = 1.9950$) that ensure finite-time synchronization. In particular, verifying that the Mittag-Leffler function $E_{0.15}(0.14905, 10)$ is below 1.5893 confirms synchronization.
- **Simulations**
  - Simulation results illustrate the evolution and synchronization of the master and slave systems over time. Specifically, Figures 1 and 2 depict the evolution of $S(n)$, $I(n)$, and $R(n)$ for the master and slave systems, while Figures 3 and 4 show the error dynamics. Figure 5 estimates the discrete Mittag-Leffler function $E_{0.14905}(0.25, t)$, confirming the synchronization condition.

This study benefits the modeling of real-world dynamics, such as the spread of COVID-19, by employing a discrete fractional-order master-slave system. By incorporating fractional derivatives, the model effectively captures memory and hereditary properties, thereby enhancing the accuracy of epidemic simulations and control strategies.

We demonstrate finite-time synchronization between the master and slave systems, a feature critical for coordinating interventions in epidemic control across different populations. Furthermore, the discrete formulation enables numerical simulations that provide insights into system behavior under diverse parameter settings, aiding policy decisions.

However, selecting inappropriate parameter values can have significant drawbacks, affecting both theoretical analysis and practical outcomes. Key disadvantages include:

- **Inaccurate Model Behavior**
  - Incorrect parameter values (e.g., for μ, $\mathfrak{d}$, or $\mathfrak{b}$) may result in unrealistic system dynamics, making it difficult to derive meaningful conclusions.
- **Failure to Achieve Synchronization**
  - Suboptimal parameter choices may prevent finite-time synchronization if values such as μ, δ, or ζ do not satisfy the conditions of Theorem 4.1, leading to instability or delayed convergence.
- **Instability in Simulations**
  - Improper values for critical parameters, such as reaction or mortality rates, may cause instability in simulations, manifesting as unbounded growth, unrealistic oscillations, or numerical divergence.
- **Unrealistic Physical Interpretations**
  - Choosing non-representative values for birth or infection rates can yield unrealistic interpretations, undermining the model's relevance to actual population dynamics.
- **Misleading Settling Time Estimates**
  - Inaccurate parameter selection may result in misleading estimates of settling time, giving false impressions of the system's stability or synchronization speed.
- **Difficulty in Replicating Results**
  - If parameters are not carefully chosen, replicating the study's results becomes challenging, which may question the robustness and scientific impact of the work.
- **Sensitivity to Small Changes**
  - Poor parameter selection can make the system overly sensitive to minor variations, leading to erratic behavior and unreliable predictions.
- **Lack of Practical Relevance**
  - Choosing values that deviate significantly from real-world scenarios can limit the model's practical relevance, reducing the applicability of the study's conclusions.
- **Suboptimal Controller Design**
  - Incorrect parameter values may lead to ineffective control laws, preventing the system from reaching the desired synchronization in practical applications.
- **Violation of Stability Conditions**
  - If parameters do not satisfy the stability conditions outlined in the theorems, the system may become unstable and unsynchronized, contradicting theoretical expectations.

These drawbacks underscore the importance of carefully choosing realistic parameter values when applying mathematical models, especially in control systems, epidemiology, and robotics.

6. Conclusion

In this study, we introduced a novel discrete FO-SIR model tailored to capture the complex transmission dynamics of COVID-19. By integrating memory effects through the Caputo fractional difference operator, our model extends classical epidemiological frameworks to incorporate nonlocal interactions and historical dependencies inherent in epidemic data. We established a master-slave system configuration and derived sufficient conditions for FTSY using the Lyapunov stability theory and the discrete Mittag–Leffler function. Numerical simulations validated our theoretical findings by demonstrating that the error dynamics between the master and slave systems converge to zero within a finite settling time under appropriately designed control strategies. These results highlight the potential of fractional calculus in enhancing the predictive accuracy of epidemic models and developing robust control strategies for coordinated interventions. Future research may extend this framework by incorporating additional epidemiological factors such as vaccination and spatial heterogeneity, thereby broadening its applicability to real-world scenarios and improving strategies for outbreak mitigation.

References

1. N. Djenina, A. Ouannas, I. M. Batiha, G. Grassi, T.-E. Oussaeif, and S. Momani, *A novel fractional-order discrete SIR model for predicting COVID-19 behavior*. Mathematics 10, 2224, (2022). doi: 10.3390/math10132224.
2. M. A. Acuña-Zegarra, S. Díaz-Infante, D. Baca-Carrasco, and D. Olmos-Liceaga, *COVID-19 optimal vaccination policies: A modeling study on efficacy, natural and vaccine-induced immunity responses*. Math. Biosci. 337, 108614, (2021).
3. F. Farooq, J. Khan, and M. U. G. Khan, *Effect of Lockdown on the spread of COVID-19 in Pakistan*. arXiv:2005.09422v1, (2020).
4. O. Iyiola, B. Oduro, T. Zabilowicz, B. Iyiola, and D. Kenes, *System of Time Fractional Models for COVID-19: Modeling, Analysis and Solutions*. Symmetry 13, 787, (2021).
5. N. H. Shah, A. H. Suthar, E. N. Jayswal, A. Sikarwar, *Fractional SIR-Model for Estimating Transmission Dynamics of COVID-19 in India*. J. 4, 86–100, (2021).
6. Z.-Y. He, A. Abbes, H. Jahanshahi, N. D. Alotaibi, and Y. Wang, *Fractional-Order Discrete-Time SIR Epidemic Model with Vaccination: Chaos and Complexity*. Mathematics 10, 165, (2022).
7. J. M. Blackledge, *On the Evolution Equation for Modelling the Covid-19 Pandemic*. In Analysis of Infectious Disease Problems (COVID-19) and Their Global Impact, P. Agarwal, J. J. Nieto, M. Ruzhansky, D. F. M. Torres, Eds., Infosys Science Foundation Series, Springer: Singapore, 2021.
8. P. Agarwal, J. J. Nieto, M. Ruzhansky, and D. F. M. Torres, *Analysis of Infectious Disease Problems (COVID-19) and Their Global Impact*. Infosys Science Foundation Series in Mathematical Sciences, Springer: Singapore, 2021.
9. N. R. Anakira, A. Almalki, D. Katatbeh, G. B. Hani, A. F. Jameel, K. S. Al Kalbani, and M. Abu-Dawas, *An algorithm for solving linear and non-linear Volterra integro-differential equations*, International Journal of Advances in Soft Computing and Its Applications, **15** (3) (2023), 77–83.
10. G. Farraj, B. Maayah, R. Khalil, and W. Beghami, *An algorithm for solving fractional differential equations using conformable optimized decomposition method*, International Journal of Advances in Soft Computing and Its Applications, **15** (1) (2023).
11. M. Berir, *Analysis of the effect of white noise on the Halvorsen system of variable-order fractional derivatives using a novel numerical method*, International Journal of Advances in Soft Computing and Its Applications, **16** (3) (2024), 294–306.
12. S. Ahmad, S. Javeed, H. Ahmad, J. Khushi, S. K. Elagan, and A. Khames, *Analysis and numerical solution of novel fractional model for dengue*. Results Phys. 28, 104669, (2021).
13. N. Djenina, G. Grassi, A. Ouannas, and Z. Dibi, *A New COVID-19 Model Using Fractional Calculus: Stability, Mitigate Pandemic And Simulations*. IFAC-PapersOnLine 58, 12, (2024). doi: 10.3390/computation12070144.
14. T. Hamadneh, A. Hioual, R. Saadeh, M. A. Abdoon, D. K. Almutairi, T. A. Khalid, and A. Ouannas, *General Methods to Synchronize Fractional Discrete Reaction-Diffusion Systems Applied to the Glycolysis Model*. Fractal Fract. 7, 11, (2023). doi: 10.3390/computation12070144.
15. A. O. Almatroud, N. Djenina, A. Ouannas, and G. Grassi, *The SEIR COVID-19 Model Described by Fractional-Order Difference Equations: Analysis and Application with Real Data in Brazil*. J. Differ. Equ. Appl. 29, 9–12, (2023). doi: 10.3390/computation12070144.
16. I. Al-Shbeil, N. Djenina, A. Jaradat, A. Al-Husban, A. Ouannas, and G. Grassi, *A New COVID-19 Pandemic Model Including the Compartment of Vaccinated Individuals: Global Stability of the Disease-Free Fixed Point*. Mathematics 11, 3, (2023). doi: 10.3390/computation12070144.
17. A. Abbes, A. Ouannas, N. Shawagfeh, and H. Jahanshahi, *The Fractional-Order Discrete COVID-19 Pandemic Model: Stability and Chaos*. Nonlinear Dyn. 111, 1, (2023). doi: 10.3390/computation12070144.

18. A. Dababneh, N. Djenina, A. Ouannas, G. Grassi, I. M. Batiha, and I. H. Jebril, *A New Incommensurate Fractional-Order Discrete COVID-19 Model with Vaccinated Individuals Compartment*. Fractal Fract. 6, 8, (2022). doi: 10.3390/computation12070144.

19. A. O. Almatroud, N. Djenina, A. Ouannas, G. Grassi, and M. M. Al-Sawalha, *A Novel Discrete-Time COVID-19 Epidemic Model Including the Compartment of Vaccinated Individuals*. Math. Biosci. Eng. 19, 1, (2022). doi: 10.3390/computation12070144.

20. N. Debbouche, A. Ouannas, I. M. Batiha, and G. Grassi, *Chaotic Dynamics in a Novel COVID-19 Pandemic Model Described by Commensurate and Incommensurate Fractional-Order Derivatives*. Nonlinear Dyn. 1, 1–13, (2021). doi: 10.3390/computation12070144.

21. K. Kozioł, R. Stanisławski, and G. Bialic, *Fractional-Order SIR Epidemic Model for Transmission Prediction of COVID-19 Disease*. Appl. Sci. 10, 8316, (2020).

22. I. M. Batiha, O. Ogilat, I. Bendib, A. Ouannas, I. H. Jebril, and N. Anakira, *Finite-Time Dynamics of the Fractional-Order Epidemic Model: Stability, Synchronization, and Simulations*. Chaos Solitons Fractals X 13, 100118, (2024). doi: 10.3390/computation12070144.

23. A. Al-Husban, N. Djenina, R. Saadeh, A. Ouannas, and G. Grassi, *A New Incommensurate Fractional-Order COVID-19 Model: Modelling and Dynamical Analysis*. Mathematics 11, 3, (2023). doi: 10.3390/computation12070144.

24. L. Xiang, Y. Zhang, and J. Huang, *Stability analysis of a discrete SIRS epidemic model with vaccination*. J. Differ. Equ. Appl. 26, 309–327, (2020).

25. M. Parsamanesh, M. Erfanian, and S. Mehrshad, *Stability and bifurcations in a discrete-time epidemic model with vaccination and vital dynamics*. BMC Bioinform. 21, 1–5, (2020).

26. M. Parsamanesh, M. Erfanian, *Stability and bifurcations in a discrete-time SIVS model with saturated incidence rate*. Chaos Solitons Fractals 150, 111178, (2021).

27. I. Abu Falahah, A. Hioual, M. O. Al-Qadri, Y. A. Al-Khassawneh, A. Al-Husban, T. Hamadneh, and A. Ouannas, *Synchronization of Fractional Partial Difference Equations via Linear Methods*. Axioms 12, 8, (2023). doi: 10.3390/computation12070144.

28. R. Hatamleh, A. Hioual, A. Qazza, R. Saadeh, and A. Ouannas, *Synchronization in Fractional Discrete Neural Networks: Constant and Variable Orders Cases*. Arab J. Basic Appl. Sci. 31, 1, (2024). doi: 10.3390/computation12070144.

29. A. Ouannas, G. Grassi, A. T. Azar, and A. A. Khennaoui, *Synchronization Control in Fractional Discrete-Time Systems with Chaotic Hidden Attractors*. Adv. Mach. Learn. Technol. Appl.: Proc. AMLTA 2020, 661–669, (2021). doi: 10.3390/computation12070144.

30. A. Ouannas, G. Grassi, A. T. Azar, A.-A. Khennaoui, and V.-T. Pham, *Synchronization of Fractional-Order Discrete-Time Chaotic Systems*. Int. Conf. Adv. Intell. Syst. Inform., 218–228, (2019). doi: 10.3390/computation12070144.

31. A. Ouannas, Z. Odibat, and N. Shawagfeh, *A New Q-S Synchronization Results for Discrete Chaotic Systems*. Differ. Equ. Dyn. Syst. 27, 4, (2019). doi: 10.3390/computation12070144.

32. A. Ouannas, L. Jouini, O. Zehrour, *On New Generalized Hybrid Synchronization in Chaotic and Hyperchaotic Discrete-Time Dynamical Systems*. J. Appl. Nonlinear Dyn. 8, 3, (2019). doi: 10.3390/computation12070144.

33. A. Ouannas, V.-T. Pham, *New Trends in Synchronization of Fractional-Order Chaotic Systems*. Handb. Fract. Calc. Appl., 397, (2019). doi: 10.3390/computation12070144.

34. I. M. Batiha, I. Bendib, A. Ouannas, I. H. Jebril, S. Alkhazaleh, S. Momani, *On New Results of Stability and Synchronization in Finite-Time for FitzHugh-Nagumo Model Using Gronwall Inequality and Lyapunov Function*. J. Robot. Control 5, 6, (2024). doi: 10.3390/computation12070144.

35. L. Jouini, A. Ouannas, *Increased and Reduced Synchronization between Discrete-Time Chaotic and Hyperchaotic Systems*. Nonlinear Dyn. Syst. Theory 19, 2, (2019). doi: 10.3390/computation12070144.

36. M. A. Hammad, I. Bendib, W. G. Alshanti, A. Alshanty, A. Ouannas, A. Hioual, S. Momani, *Fractional-Order Degn–Harrison Reaction–Diffusion Model: Finite Time Dynamics of Stability and Synchronization*. Computation 12, 144, (2023). doi: 10.3390/computation12070144.

37. W. Pan, T. Li, *Finite-Time Synchronization of Fractional-Order Chaotic Systems with Different Structures under Stochastic Disturbances*. J. Comput. Commun. 9, 120–137, (2021). doi: 10.4236/jcc.2021.96007.

38. H. M. Almimi, M. Abu Hammad, G. Farraj, I. Bendib, A. Ouannas, *A New Investigation on Dynamics of the Fractional Lengyel-Epstein Model: Finite Time Stability and Finite Time Synchronization*. Computation 12, 197, (2024). doi: 10.3390/computation12100197.

39. S. Momani, I. M. Batiha, I. Bendib, A. Ouannas, A. Hioual, D. Mohamed, *Examining finite-time behaviors in the fractional Gray-Scott model: Stability, synchronization, and simulation analysis*. Int. J. Cogn. Comput. Eng.

40. F. Liu, S. Huang, S. Zheng, H. O. Wang, *Stability Analysis and Bifurcation Control for a Fractional Order SIR Epidemic Model with Delay*. In Proceedings of the 2020 39th Chinese Control Conference (CCC), Shenyang, China, 27–29 July 2020, pp. 724–729.

41. I. M. Batiha, S. Momani, A. Ouannas, Z. Momani, S. B. Hadid, *Fractional-order COVID-19 pandemic outbreak: Modeling and stability analysis*. Int. J. Biomath. 15, 2150090, (2021).

42. O. A. Almatroud, I. Bendib, A. Hioual, A. Ouannas, *On stability of a reaction-diffusion system described by difference equations*. J. Differ. Equ. Appl. 1-15, (2024).

43. I. Bendib, I. M. Batiha, A. Hioual, N. Anakira, M. Dalah, A. Ouannas, *On a new version of the Gierer-Meinhardt model using fractional discrete calculus*. Results Nonlinear Anal. 7(2), 1-15, (2024).

44. T. Abdeljawad, *On Riemann and Caputo fractional differences*. Comput. Math. Appl. 62, 1602–1611, (2011).

45. G.-C. Wu, D. Baleanu, S.-D. Zeng, *Finite–time stability of discrete fractional delay systems: Gronwall inequality and stability criterion*. Commun. Nonlinear Sci. Numer. Simul., (2017). doi: 10.1016/j.cnsns.2017.09.001.

46. A. Abdurahman, H. Jiang, Z. Teng, *Finite-time synchronization for fuzzy cellular neural networks with time-varying delays*. Fuzzy Sets Syst. 297, 96–111, (2016).

47. S. Zhao, K. Li, W. Hu, Y. Wang, *Finite-time synchronization of discontinuous fuzzy neural networks with mixed time-varying delays and impulsive disturbances*. Results Control Optim. 12, 100253, (2023). doi: 10.1016/j.rico.2023.100253.

[1] *Department of Mathematics, Al Zaytoonah University, Amman 11733, Jordan*

[2] *Nonlinear Dynamics Research Center (NDRC), Ajman University, Ajman 346, UAE*

E-mail address: i.batiha@zuj.edu.jo

and

[3] *Department of Mathematics, Faculty of Exact Sciences, University of Brothers Mentouri, Constantine 25000, Algeria*

E-mail address: bendib.issam@doc.umc.edu.dz

and

[4] *Department of Mathematics and Computer Science, University of Oum EL-Bouaghi, Oum EL-Bouaghi, Algeria*

E-mail address: ouannas.adel@univ-oeb.dz

and

[5] *Department of Mathematics, Anand International College of Engineering, Jaipur 303012, India*

E-mail address: goyal.praveen2011@gmail.com

and

[6] *Faculty of Education and Arts, Sohar University, Sohar 3111, Oman*

E-mail address: nanakira@su.edu.om

and

[7] *Applied Science Research Center, Applied Science Private University, Amman 11937, Jordan*

and

[8] *Department of Mathematics, The University of Jordan, Amman, Jordan*

E-mail address: s.momani@ju.edu.jo